A Giant Flare from a Soft Gamma Repeater in the Andromeda Galaxy, M31

E. P. Mazets[1], R. L. Aptekar[1], T. L. Cline[2], D. D. Frederiks[1], J. O. Goldsten[3], S. V. Golenetskii[1], K. Hurley[4], A. von Kienlin[5], and V. D. Pal'shin[1]

ABSTRACT

The light curve, energy spectra, energetics, and IPN localization of an exceedingly intense short duration hard spectrum burst, GRB 070201, obtained from Konus-Wind, INTEGRAL (SPI-ACS), and MESSENGER data are presented. The total fluence of the burst and the peak flux are $S = 2.00^{+0.10}_{-0.26} \times 10^{-5}$ erg cm^{-2} and $F_{\max} = 1.61^{+0.29}_{-0.50} \times 10^{-3}$ erg cm^{-2} s^{-1}. The IPN error box has an area of 446 square arcminutes and covers the peripheral part of the M31 galaxy. Assuming that the source of the burst is indeed in M31 at a distance of 0.78 Mpc, the measured values of the fluence S and maximum flux $F_{\max}$ correspond to a total energy of $Q = 1.5 \times 10^{45}$ erg, and a maximum luminosity $L = 1.2 \times 10^{47}$ erg s^{-1}. These data are in good agreement with the corresponding characteristics of the previously observed giant flares from other soft gamma repeaters. The evidence for the identification of this event as a giant flare from a soft gamma repeater in the M31 galaxy is presented.

Subject headings: gamma-ray bursts; soft gamma-ray repeaters

1. INTRODUCTION

Soft gamma repeaters (SGRs) are a special rare class of strongly magnetized neutron stars exhibiting two types of gamma-ray burst emission. Occasionally, SGRs enter an active stage and emit repeated short bursts with spectra which in an energy range above 10–15 keV can be approximated by a soft thermal bremsstrahlung-like function with $kT \approx 20$–30 keV. The bursting activity may last from several days to a year or more, followed by a long quiescent period lasting up to several years.

Much more rarely, perhaps once every 30–40 years, an SGR may emit a giant flare (GF) with enormous intensity. The energy released in such a flare in gamma-rays is comparable to the total

---

[1]Ioffe Physico-Technical Institute of the Russian Academy of Sciences, St. Petersburg, 194021, Russia

[2]Goddard Space Flight Center, NASA, Greenbelt, MD 20771, USA

[3]The Johns Hopkins University Applied Physics Laboratory, MD 20723, USA

[4]Space Sciences Laboratory, University of California at Berkeley, Berkeley, CA 94720-7450, USA

[5]Max-Plank-Institut für extraterrestrische Physik, D-85741 Garching, Germany

energy emitted by the Sun over 10^4–10^5 years or more. GFs display short ($\sim$ 0.2–0.5 s) initial pulses of hard gamma rays with a steep leading edge and a more extended trailing edge which as a rule evolves into a soft long decaying tail pulsating with the neutron star rotation period. A GF is frequently preceded by pronounced increase in bursting activity (Frederiks et al. 2007a).

The first two SGRs were discovered and localized in March, 1979 by the Konus experiment on Venera 11 and 12. A giant flare from SGR 0526-66 was detected on March 5, 1979 by numerous spacecraft (Mazets et al. 1979a; Evans et al. 1980; Cline et al. 1980). One of the first results of the interplanetary network (IPN) was the localization of the first GF to an error box inside the N49 supernova remnant in the Large Magellanic Cloud (LMC) (Cline et al. 1980). Another important result was the observation and localization by the Konus experiment of $\sim$17 weak soft recurrent bursts emitted by SGR 0526-66 in the years following the GF (Mazets et al. 1979a; Golenetskii et al. 1984). Moreover, in 1979 March, Konus detected and localized three similar recurrent bursts from another source, SGR 1900+14 (Mazets et al. 1979b). The third SGR, 1806-20, was discovered in 1983 (Laros et al. 1987; Atteia et al. 1987; Kouveliotou et al. 1987), and the fourth, SGR 1627-41, in 1998 (Hurley et al. 1999b; Woods et al. 1999). It has become clear that SGRs are very rare astrophysical objects. The giant flare on 1979 March 5 remained a unique event for 20 years, until new giant flares were detected from SGR 1627-41 on 1998 June 18 (Mazets et al. 1999a) and from SGR 1900+14 on 1998 August 27 (Hurley et al. 1999a; Feroci et al. 1999; Mazets et al. 1999b). Finally, a giant flare from SGR 1806-20 on December 27, 2004 was also observed (Hurley et al. 2005; Frederiks et al. 2007a). The extremely high intensity of the initial pulses of the giant flares suggested that these events could be detected in galaxies at distances up to 10–30 Mpc.

The short hard GRB 051103 was localized by the interplanetary network to the nearby M81 group of interacting galaxies which lies at a distance of 3.6 Mpc (Golenetskii et al. 2005). The possibility of identifying this burst as a GF from an SGR in the M81 group, as opposed to a short GRB in a background galaxy, has been discussed (Frederiks et al. 2007b; Hurley et al. 2007a).

On 2007 February 1 Konus-Wind recorded a short duration hard spectrum gamma-ray burst which had a higher intensity than any previously observed event. The burst was localized by the IPN (Golenetskii et al. 2007). The final localization (a 446 arcmin^2 error box) covers the outer arms of the M31 galaxy. The analysis presented below of the time history, spectral characteristics, and energetics argues strongly for the interpretation that this event is actually a GF from a soft gamma repeater in the Andromeda galaxy. In a companion paper, Abbott et al. (2007) discuss the LIGO data taken at the time of this event.

2. OBSERVATIONS AND LOCALIZATION

The light curve of GRB 070201 (Konus trigger time T_0=55390.780 s UT, corresponding to an Earth-crossing time 55390.261 s) recorded by the Konus-Wind S2 detector in the energy range 17–1130 keV is shown in Fig. 1. It displays a narrow pulse with a rather steep leading edge ($\sim$20 ms)

followed by more prolonged decay to T-$T_0 \approx 180$ ms. The maximum count rate occurs in a ≤ 2 ms long interval. The burst profile is not smooth: in most cases, the variations evident in the count rate at the top of the pulse and in its decay phase are statistically significant. A weak secondary flash is observed at T-$T_0 \approx 180$–280 ms. Comparison of the light curves in three energy bands G1 (17–70 keV), G2 (70–300 keV), and G3 (300–1130 keV) (Fig. 2) and of the hardness ratios G2/G1 and G3/G2 reveals a strong, rapid spectral evolution of the radiation. The most pronounced changes are observed for the high-energy part of the spectrum (energies $E_\gamma > 300$ keV). The duration of the high-energy radiation does not exceed 80 ms. The second, weak rise in intensity at T-$T_0 \approx 180$ ms is present only for the soft part of the spectrum at energies $E_\gamma < 300$ keV. Four multichannel spectra were measured in the course of the burst, each with an accumulation time of 64 ms. They cover the energy range from 17 keV to 14 MeV, but no statistically significant emission is seen above 2 MeV. The boundaries of the successive accumulation intervals N=1, 2, 3, and 4 are shown in Fig. 2 by dashed vertical lines. Because of the small number of counts in interval 3, spectra 3 and 4 were combined. The time-integrated spectrum of the entire burst was accumulated over the interval 0–256 ms. The raw count rate spectra were rebinned in order to have at least 20 counts per energy bin and then fitted using XSPEC, version 11.3 (Arnaud 1996). The detector response function was calculated specifically for the 55°9 burst incidence angle, determined from the IPN localization data.

A good fit was obtained for a power-law spectrum with an exponential cutoff, $dN_{ph}/dE \propto E^{-\alpha} \exp\left[-(2-\alpha)E/E_p\right]$, where E_p is the peak energy in the $EF(E)$ spectrum. We also tested the Band (GRRM) model but no statistically significant high energy power-law tail was found in any fitted spectrum. The deconvolved photon spectra for the intervals 1, 2, and 3+4, and for the time-integrated spectrum of the burst, are shown in Fig. 3, and the spectral parameters are summarized in Table 1. Comparison of the E_p values shows that the spectrum for interval 1 is the hardest. Returning to Fig. 2, note that the accumulation time of this spectrum is rather long (64 ms) compared to the characteristic evolution time and hence the spectrum is strongly time-averaged. Most of the high-energy photons are accumulated during the first ~ 20 ms. This remarkable fact means that the flux of photons with the hardest spectrum is emitted near the peak of the initial pulse. The burst fluence in the 20 keV-1.2 MeV range is $2.00^{+0.10}_{-0.26} \times 10^{-5}$ erg cm^{-2}. The 2-ms peak flux measured from $T_0+0.016$ s in the same energy band is $1.61^{+0.29}_{-0.50} \times 10^{-3}$ erg cm^{-2} s^{-1}. All the uncertainties are for the 90% confidence level.

GRB 070201 was detected by Wind (Konus) with a time resolution of up to 2 ms, by INTEGRAL (SPI-ACS) with a resolution of 50 ms, by MESSENGER (MErcury Surface, Space ENvironment, GEochemistry, and Ranging , Gamma-Ray and Neutron Spectrometer, Goldsten et al. (2007)) with a resolution of 1 s, and by the Swift BAT with 1 s resolution (outside the coded field of view, J. Cummings, private communication 2007). The initial triangulation was given in Hurley et al. (2007b). The coordinates of the center and vertices of the refined 446 arcmin^2 3σ error box are listed in Table 2. The center lies $\sim 1°$ away from the center of M31. Assuming that the source of GRB 070201 is situated in M31 at a distance of 0.78 Mpc, the measured values of the

fluence and peak flux correspond to an isotropic energy output $Q = 1.5 \times 10^{45}$ erg, and an isotropic peak luminosity $L = 1.2 \times 10^{47}$ erg s^{-1}.

The relative proximity of M31 makes it worthwhile to search for the afterglow of GRB 070201 in soft gamma rays, i.e., the tail of the possible giant flare. While recording a burst in the trigger mode with high time resolution, Konus also continues to measure the count rates in each of the detectors S1 and S2 in four energy windows G1, G2, G3, and Z (a charged particles channel) in background mode with a time resolution of 2.944 s. The initial pulse of GRB 070201 falls completely in a single 2.944 s interval around T_0. We began by selecting a long series of count rate data, excluding this interval. Then, in order to suppress fast statistical fluctuations we formed a new series consisting of a sum over 94.2 s (32×2.944s), which can originate at the beginning of any 2.944 s interval. Two such series, in the energy bands G1 and G2, are shown in Figures 4a and b; they are synchronized to the first 2.944 s interval following the excluded one. The position of the excluded interval is marked by a narrow vertical line. The discontinuity at T-T_0 ∼240–3800 s is due to the transfer of the accumulated data to the on-board memory. A significant increase in the count rate (4.3σ above the average background level) is seen only in the soft energy band G1 and only for the first large interval after T_0. Panel 4c shows how the excess counts ΔN vary if the beginning of the 94.2 s interval is shifted forwards or backwards from T_0 step-by-step by 2.944 s. The dependence of ΔN on the time shift ΔT implies that the gradually decreasing soft gamma-ray flux is indeed present in each 2.944 s interval after T_0 but is absent prior to it. This important result confirms the detection of the decaying soft afterglow of GRB 070201. For an OTTB spectrum with $kT \approx 30$ keV, the 94.2 s count excess $\Delta N = 1385 \pm 320$ corresponds to a fluence $S \approx 1 \times 10^{-6}$ erg cm^{-2}. Assuming that we are observing emission in the tail of a GF from M31, its energy is $Q_{\text{tail}} \approx 7 \times 10^{43}$ erg.

3. DISCUSSION

The Andromeda galaxy, M31, as the closest massive galaxy, has long been regarded as one of the most likely candidates for searching for observable GFs from distant extragalactic SGRs (Mazets et al. 1999b; Bisnovatyi-Kogan 1999). It is well known that one of the dominant features of the structure of M31 is a bright circular ring with a radius of 10 kpc discovered by Arp (1964) in Hα observations. In agreement with numerous observations, the ring reveals the main star-formation region of the galaxy. In the far infrared, the first *IRAS* images of M31 also revealed a bright circular ring (Habing et al. 1984). The close correspondence between the details of the Hα and far infrared images of the galaxy implies that the radiation of massive hot stars (Devereux et al. 1994) is the common energy source of these emissions. Recently, high spatial resolution images of M31 have been obtained in the mid- and far infrared at different wavelengths with the *Spitzer* space telescope (Barmby et al. 2006; Gordon et al. 2006) and in the far and near ultraviolet with *GALEX* (Thilker et al. 2005). These very similar images clearly show the central region, the fragmented spiral arms, the main circular ring with $R \approx 10$ kpc, and a less luminous outer ring with $R \approx 14$ kpc.

Figure 5 shows the UV image of M31 (Thilker et al. 2005). The IPN error box overlaps the

northeastern part of the galaxy. It contains segments of both the $R \approx 10$ kpc ring and of the weaker $R \approx 14$ kpc outer ring. The probability of a chance overlapping of the error box and the image is rather low ($\sim 10^{-4}$). Twenty-two sources from an *XMM-Newton* X-ray survey of M31 (Pietsch et al. 2005) fall within the error box. Among these, two sources are active galaxy nuclei (AGN) and five are foreground objects. SGRs in the quiescent state are typically sources of pulsating soft X-rays with an average 0.5–10 keV luminosity of 10^{35}–10^{36} erg s^{-1} and a spectrum which can be described as a combination of a blackbody and power law (Kulkarni et al. 2003; Hurley et al. 2000; Kouveliotou et al. 2001). Spectral studies of the unidentified soft X-ray sources in the error box which could be SGRs in M31 would clearly be important.

We now examine additional evidence which strengthens the interpretation of the 2007 February 1 event as a GF from an SGR in M31. This comes from a comparison of the energetics, time history, and spectral behavior of GRB 070201 with the corresponding characteristics of the previously observed giant flares on 1979 March 5 (SGR 0525-66), 1998 June 18 (SGR 1627-41), 1998 August 27 (SGR 1900+14), and 2004 December 27 (SGR 1806-20). Here we are mainly interested in the characteristics of the GF initial pulses, but unfortunately, it is just this information which is the hardest to obtain reliably. When a sensitive gamma-ray detector records an initial pulse with an immense intensity, it is strongly overloaded, which makes it difficult or even impossible to obtain information about the main part of the peak. If a giant pulse is recorded by detectors of low-energy charged particles which have low sensitivity to gamma-rays, there is no saturation problem in most cases. However, severe difficulties are encountered instead when measuring the photon energy, obtaining spectra, and consequently deriving energy estimates. Nevertheless, the entire set of data on initial pulses, obtained both with gamma-ray spectrometers (Mazets et al. 1979a, 1982; Hurley et al. 1999a; Mazets et al. 1999a; Frederiks et al. 2007a) and with charged-particle detectors (Hurley et al. 2005; Palmer et al. 2005; Terasawa et al. 2005; Schwartz et al. 2005; Tanaka et al. 2007), can be used to establish the general pattern of the initial pulse.

We will restrict this comparison of GFs to a limited number of their characteristics, for the following reasons. The time structure of the initial pulse is likely to be very complex. The profile of both the steep leading edge of the pulse, as in SGR 1806-20 (Palmer et al. 2005), and its more prolonged decay, as in SGR 1900+14 (Tanaka et al. 2007), contain significant intensity variations on both short and long timescales. Among other things, the appearance of the light curve will be strongly affected by the spectral variability of the emission. At high count rates close to saturation level, dead-time and pileup corrections of light curves and energy spectra are difficult, if not impossible. Therefore, we include in Table 3 only two fairly reliable characteristics of the initial pulse, t_R and E_p; t_R, the rise time, is the time between the detection of hard gamma-radiation above the background to the peak of the initial pulse, E_p is the photon energy at the maximum of the time-integrated $EF(E)$ spectrum of the pulse. Table 3 also contains data on the peak luminosity $L_{\max}$ and the energy release Q of the initial pulses, as well as the energy in the GF tails Q_{tail}. In keeping with tradition, we suggest the same nomenclature for extragalactic and galactic SGRs, namely SGR followed by the coordinates (α, δ) of the center of the error box.

Table 3 shows that estimates of both the luminosities and energy outputs in GFs are spread over a range of several orders of magnitude. On the other hand, the values of Q_{tail} are practically equal. Thus it is particularly significant that the afterglow of GRB 070201 is similar to those of the other SGRs. A small spread in SGR Q_{tail} values implies similar magnetic field strengths, from confinement arguments (Thompson & Duncan 1995). The only exception so far is the absence of a tail in GF 980618 from SGR 1627-41, which is probably caused by the relative weakness of the magnetic field or its orientation. On the whole, Table 3 clearly demonstrates that both the temporal and energetic characteristics of the event on 2007 February 1 match the general pattern of a giant flare very closely. Beyond a doubt, we can conclude that this event is a GF which originated in SGR 0044+42 in M31.

REFERENCES

Abbott, B., et al. 2007, ApJ, submitted (astro-ph/0711.1163)

Aptekar, R. L., et al. 2001, ApJS, 137, 222

Arnaud, K. A. 1996, in ASP Conf. Ser. 101, Astronomical Data Analysis Software and Systems V, ed. G. Jacoby, & J. Barnes, (San Francisco: ASP), 17

Arp, H., et al. 1964, ApJ, 139, 1045

Atteia, J-L., et al. 1987, ApJ, 320, L105

Barmby, P., et al. 2006, ApJ, 650, L45

Bisnovatyi-Kogan, G. S. 1999, preprint (astro-ph/9911275)

Cline,T., et. al. 1980, ApJ, 237, L1

Devereux, N. A., et al. 1994, AJ, 108, 1667

Evans, W. D., et al. 1980, ApJ, 237, L7

Feroci, M., et al. 1999, ApJ, 515, L9

Frederiks, D. D., et al. 2007a, Astronomy Letters, 33, 1

Frederiks, D. D., et al. 2007b, Astronomy Lettrs, 33, 19

Goldsten, J., et al. 2007, Space Sci. Rev., 131, 339

Golenetskii, S. V., et al. 1984, Nature, 307, 41

Golenetskii, S. V., et al. 2005, GCN Circular 4197

Golenetskii, S. V., et al. 2007, GCN Circular 6088

Gordon, K. D., et al. 2006, ApJ, 638, L87

Habing, H. J., et al. 1984, ApJ, 278, L59

Hurley, K., et al. 1999a, Nature, 397, 41

Hurley, K., et al. 1999b, ApJ, 519, L143

Hurley, K., et al. 2000, in Gamma-Ray Bursts: 5th Huntsville Symp., ed. R. M. Kippen, R. S., Mallozi, & G. F. Fishman (Melville: AIP), 763

Hurley, K., et al. 2005, Nature, 434, 1098

Hurley, K., et al. 2007a, in preparation

Hurley, K., et al. 2007b, GCN Circular 6103

Kouveliotou, C., et al. 1987, ApJ, 322, L21

Kouveliotou, C., et al. 2001, ApJ, 558, L47

Kulkarni, S. R., et al. 2003, ApJ, 585, 948

Laros, J. L., et al. 1987, ApJ, 320, L111

Mazets, E. P., et al. 1979a, Nature, 282, 587

Mazets, E. P., et al. 1979b, Sov. Astron. Lett., 5(6), 343

Mazets, E. P., Golenetskii, S. V., Guryan, Yu. A., & Ilyinskii, V. N. 1982, Ap&SS, 84, 173

Mazets, E. P., et al. 1999a, ApJ, 519, L151

Mazets, E. P., et al. 1999b, Astronomy Letters, 25, 73

Palmer, D. M., et al. 2005, Nature, 434, 1107

Pietsch, W., Freyberg, M., & Haberl, F. 2005, A&A, 434, 483

Schwartz, S. J., et al. 2005, ApJ, 627, L129

Tanaka, Y. T., et al. 2007, ApJ, 665, L55

Thompson, C., & Duncan, R. 1995, MNRAS, 275, 255

Terasawa, T., et al. 2005, Nature, 434, 1110

Thilker, D. A., et al. 2005, ApJ, 619, L67
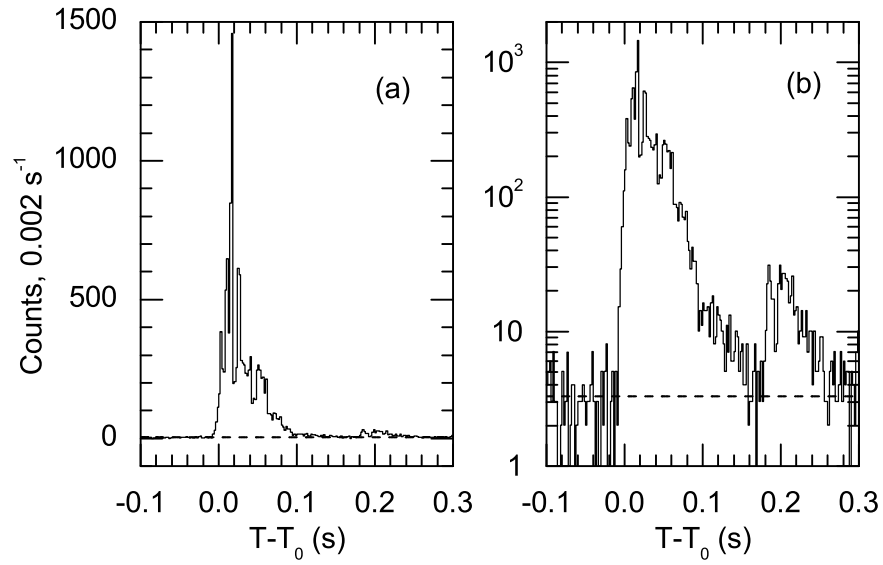
Woods, P. M., et al. 1999, ApJ, 519, L139

Fig. 1.— 17–1130 keV Konus-Wind light curve of GRB 070201 (dead time corrected) at the highest available time resolution (2 ms) presented on a linear count rate scale (a), and also on a logarithmic scale (b) to enhance the low-intensity portions.
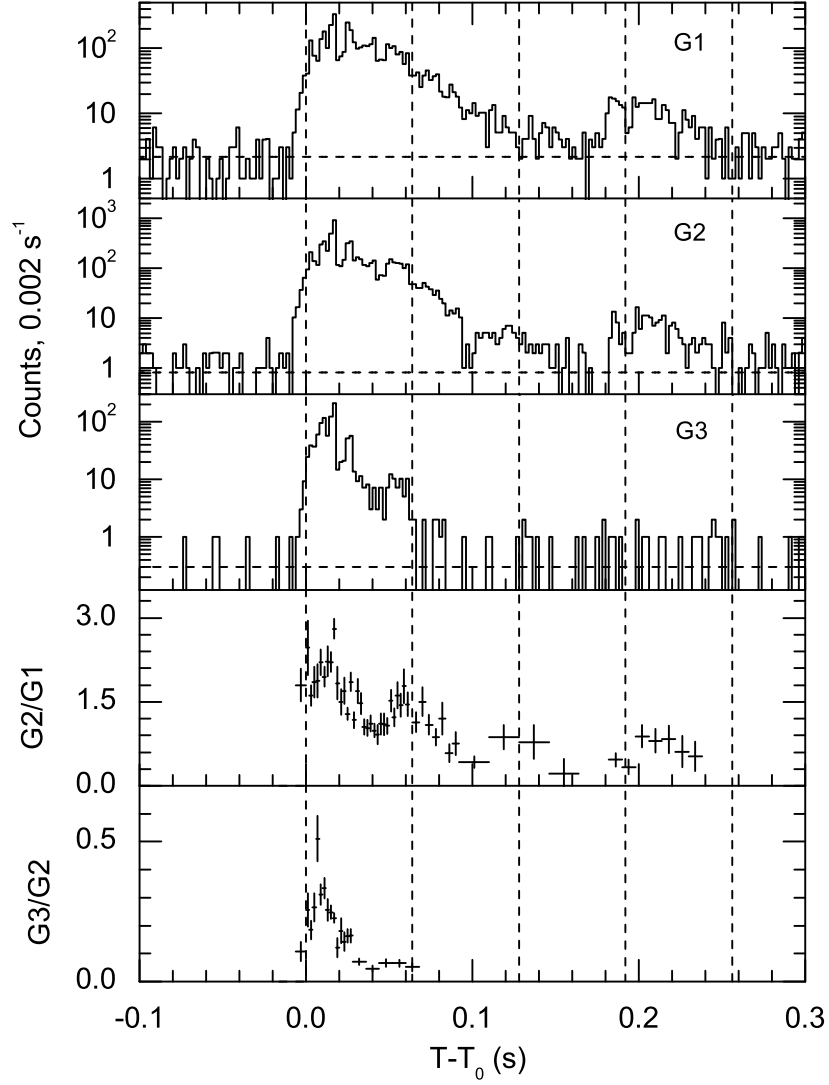
Fig. 2.— Konus-Wind light curve in three energy bands: G1 (17–70 keV), G2 (70–300 keV), and G3 (300–1130 keV), and the hardness ratios G2/G1 and G3/G2. The vertical dashed lines indicate the four successive 64-ms intervals where the energy spectra were measured.
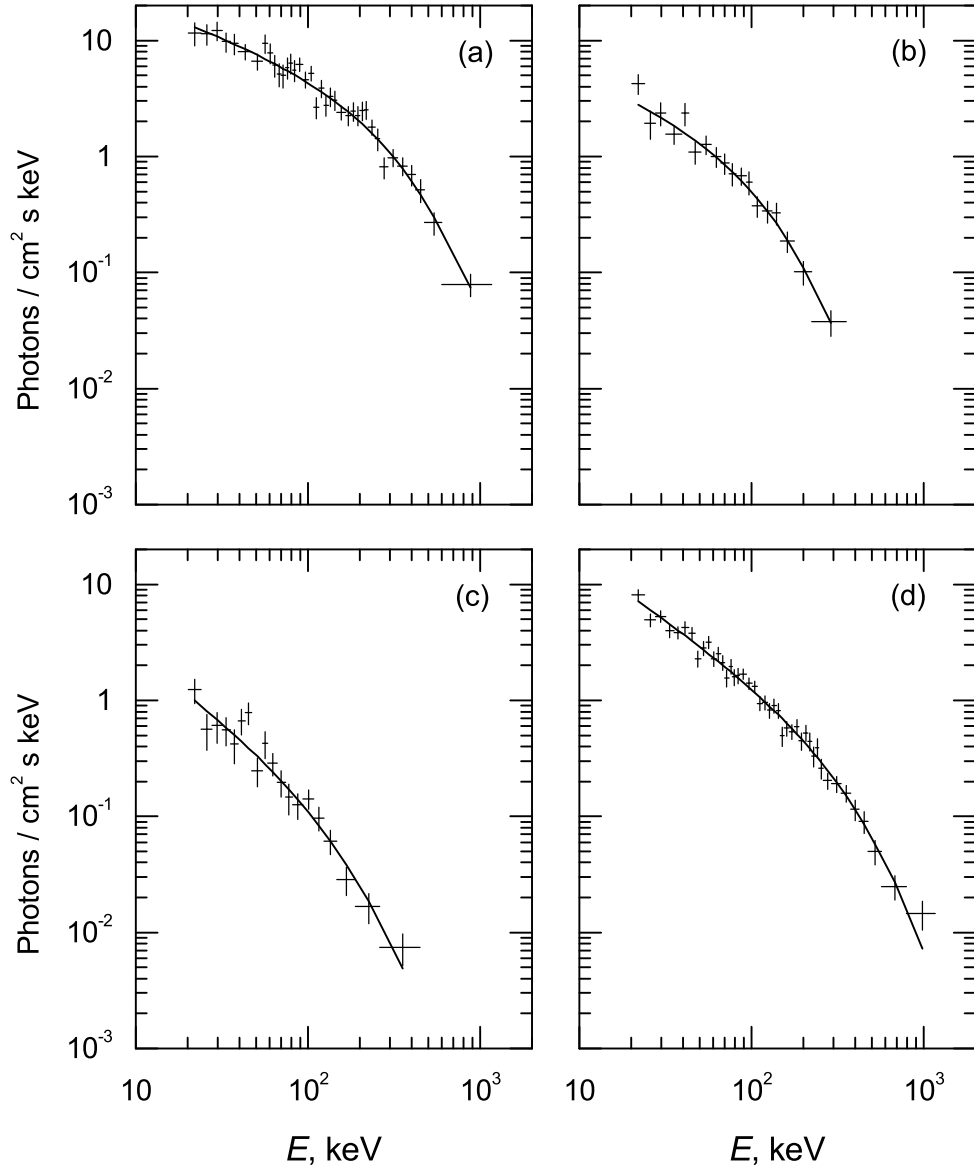
Fig. 3.— Deconvolved photon spectra of the burst accumulated over the $(T-T_0)$ intervals 0-64 ms (a), 64-128 ms (b), 128-256 ms (c), and the time-integrated spectrum, 0-256 ms (d).
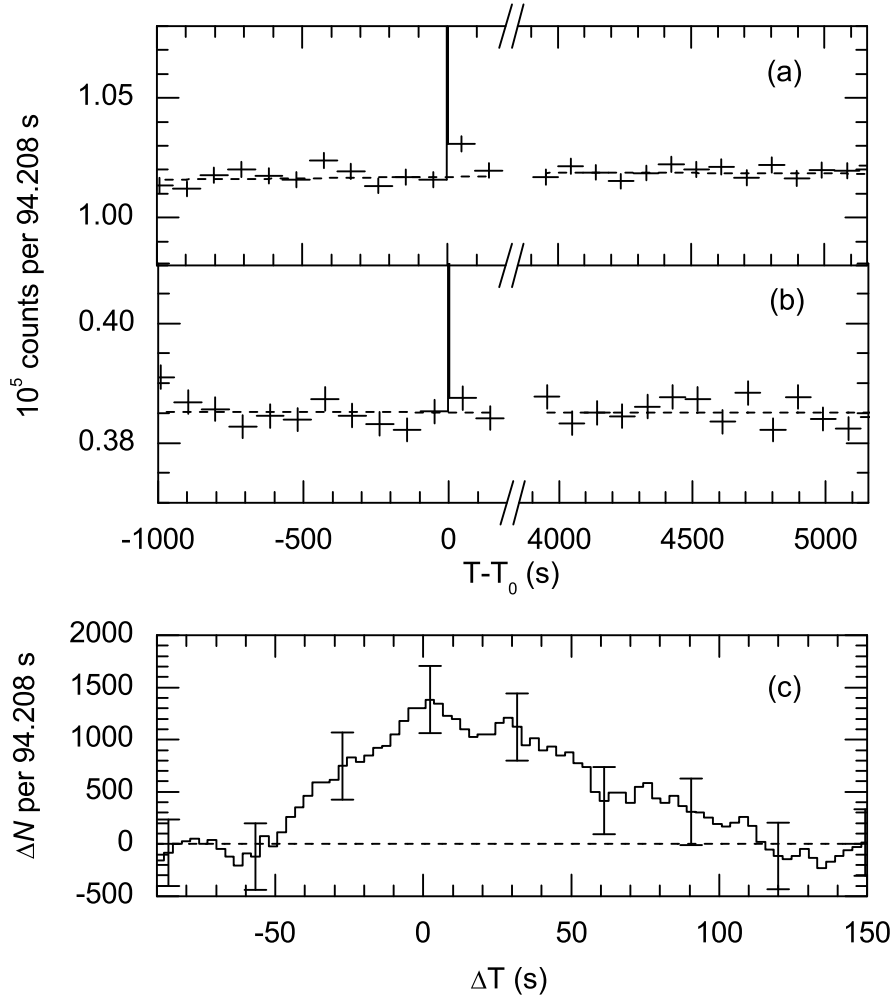
Fig. 4.— Waiting mode count rates N in the energy bands G1 (a) and G2 (b) averaged over 94.208 s intervals (excluding the burst). For G1, the first interval after T_0 exhibits a count excess ΔN of 4.3σ above the average background level. The bottom panel (c) shows how this excess ΔN varies if the beginning of the 94.208-interval is shifted by an interval ΔT forwards or backwards from T_0 step by step, with $\Delta T = 2.944$ s.
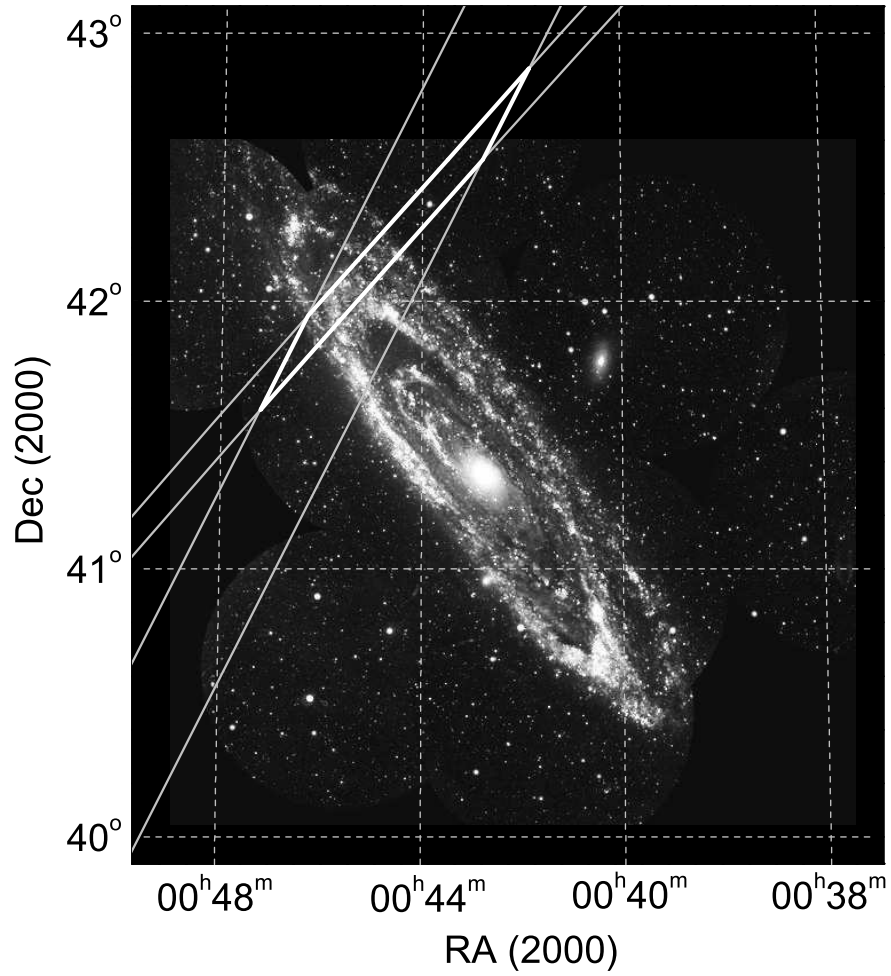
Fig. 5.— UV image of the M31 galaxy (Thilker et al. 2005) and the 3σ IPN error box of GRB 070201.

Table 1. Summary of spectral fits

Time interval (s)	α	E_p (keV)	χ^2/dof
0–0.064	$0.52^{+0.13}_{-0.15}$	360^{+44}_{-38}	31.6/35
0.064–0.128	$0.56^{+0.38}_{-0.42}$	128^{+24}_{-16}	11.3/15
0.128–0.256	$1.06^{+0.42}_{-0.52}$	123^{+54}_{-25}	19.3/16
0–0.256	$0.98^{+0.10}_{-0.11}$	296^{+38}_{-32}	39.7/40

Table 2. IPN error box of GRB 070201

	RA(2000)	Dec(2000)
Center	$00^\mathrm{h}44^\mathrm{m}32^\mathrm{s}$	$+42°14'21''$
Vertices		
1	$00^\mathrm{h}46^\mathrm{m}18^\mathrm{s}$	$+41°56'42''$
2	$00^\mathrm{h}41^\mathrm{m}51^\mathrm{s}$	$+42°52'08''$
3	$00^\mathrm{h}42^\mathrm{m}47^\mathrm{s}$	$+42°31'41''$
4	$00^\mathrm{h}47^\mathrm{m}14^\mathrm{s}$	$+41°35'35''$

Table 3.   Some characteristics of known giant flares

	SGR 0526-66[a] (LMC)	SGR 1627-41[b]	SGR 1900+14[c]	SGR 1806-20[d]	SGR 0952+69[e] (M81)	SGR 0044+42[f] (M31)
Data, YYMMDD	790305	980618	980827	041227	051103	070201
Distance, kpc	50	10	15	15	3600	780
Rise time, t_R, ms	~ 25	~ 15	~ 15	~ 25	~ 6	~ 20
Peak energy, E_p, keV	~ 500	~ 150	> 250	~ 850	~ 900	~ 300
Luminosity, $L_{\max}$, erg s^{-1}	6.5×10^{45}	3.4×10^{44}	2.3×10^{46}	3.5×10^{47}	4.3×10^{48}	1.2×10^{47}
Energy release, Q, erg	7×10^{44}	1×10^{43}	4.3×10^{44}	2.3×10^{46}	7×10^{46}	1.5×10^{45}
Tail energy, Q_{tail}, erg	3.6×10^{44}	absent	1.2×10^{44}	2.1×10^{44}	not detected	7×10^{43}

[a]The previous dead-time correction for the event (Mazets et al. 1979a, 1982) has been revised here, assuming that the initial pulse displays the expected strong hard-to-soft spectral evolution. This resulted in a reduction in t_R and an increase in $L_{\max}$ and Q.

[b]Mazets et al. (1999a); Aptekar et al. (2001).

[c]Tanaka et al. (2007); Hurley et al. (1999a); Mazets et al. (1999b).

[d]Palmer et al. (2005); Frederiks et al. (2007a).

[e]Frederiks et al. (2007b).

[f]This work.